

Dynamics of coding in communicating with chaos

Erik Bolt¹ and Ying-Cheng Lai²

¹*Department of Mathematics, 572 Holloway Road, United States Naval Academy, Annapolis, Maryland 21402-5002*

²*Department of Physics and Astronomy and Department of Mathematics, The University of Kansas, Lawrence, Kansas 66045*

(Received 14 November 1997; revised manuscript received 5 March 1998)

Recent work has considered the possibility of utilizing symbolic representations of controlled chaotic orbits for communicating with chaotically behaving signal generators. The success of this type of nonlinear digital communication scheme relies on partitioning the phase space properly so that a good symbolic dynamics can be defined. A central problem is then how to encode an arbitrary message into the wave form generated by the chaotic oscillator, based on the symbolic dynamics. We argue that, in general, a coding scheme for communication leads to, in the phase space, restricted chaotic trajectories that live on nonattracting chaotic saddles embedded in the chaotic attractor. The symbolic dynamics of the chaotic saddle can be robust against noise when the saddle has large noise-resisting gaps covering the phase-space partition. Nevertheless, the topological entropy of such a chaotic saddle, or the channel capacity in utilizing the saddle for communication, is often less than that of the chaotic attractor. We present numerical evidences and theoretical analyses that indicate that the channel capacity associated with the chaotic saddle is generally a nonincreasing, devil's-staircase-like function of the noise-resisting strength. There is usually a range for the noise strength in which the channel capacity decreases only slightly from that of the chaotic attractor. The main conclusion is that nonlinear digital communication using chaos can yield a substantial channel capacity even in noisy environment.

[S1063-651X(98)04708-4]

PACS number(s): 05.45.+b

I. INTRODUCTION

Digital communication plays an extremely important role in a modern economy. At present, digital communication is carried out mainly by linear devices, that is, by transmitters and receivers operating in the linear regime. Recent development in nonlinear dynamics and chaos has led to the idea of realizing digital communication by utilizing devices operating in nonlinear regimes [1,2]. Specifically, it has been demonstrated both theoretically [1] and experimentally [2] that a chaotic system can be manipulated, via arbitrarily small time-dependent perturbations, to generate controlled chaotic orbits whose symbolic representation corresponds to the digital representation of a desirable message. Imagine a chaotic oscillator that generates a large amplitude signal consisting of an apparently random sequence of positive and negative peaks. A possible way to assign a symbolic representation to the signal is to associate a positive peak with a one, and a negative peak with a zero, thereby generating a binary sequence. The use of small perturbations to an accessible system parameter or variable can then cause the signal to follow an orbit whose binary sequence encodes a desirable message that one wishes to transmit [1,2]. One advantage of this type of communication strategy is that the nonlinear chaotic oscillator that generates the wave form for transmission can remain simple and efficient, while all the necessary electronics controlling encoding of the signal remain at low-powered microelectronic level.

A central issue in any digital communication devices is to select a proper coding scheme by which arbitrary messages can be encoded into the transmitting signal. The main purpose of this paper is to study the dynamics of coding in nonlinear digital communicating with chaos. Assuming that the nonlinear device to be used for information encoding

generates a chaotic attractor in the phase space, we address the following questions: (1) What type of chaotic trajectories or dynamical invariant sets does a general coding scheme generate? (2) How much information can be transmitted via a chaotic oscillator through a coding? (3) What is the influence of noise on coding? The answers to these questions constitute an essential step in the development of a general theoretical framework and practical designing criteria for nonlinear digital communication with chaos.

The first result of this paper is that, in general, a coding scheme generates chaotic trajectories that live on one of the uncountably infinite number of nonattracting chaotic saddles embedded in the chaotic attractor. To understand this, imagine the two-symbol (0 and 1) case and assume that we consider an n -bit symbol sequences. For a nonlinear oscillator that generates a chaotic attractor, if the dynamics corresponds to a Bernoulli shift, there are 2^n possible symbol sequences. The number of allowed n -bit symbol sequences in most chaotic oscillators is usually less than 2^n : the allowed ones are called the grammar. That is, there are always forbidden symbol sequences. In communication, however, the binary representation of a message to be transmitted may contain all possible symbol sequences. Thus, it is necessary to code the message so that its encoded binary representation constitutes symbol sequences that are allowed by the grammar of the chaotic oscillator. In practice, it is difficult to design a code that excludes only the forbidden symbol sequences. Given a code, the set of excluded symbol sequences usually includes a number of symbol sequences that are actually allowed by the grammar. Thus, it is often the case that only a subset of all the allowed symbol sequences is utilized. Since all the allowed symbol sequences correspond to the original chaotic attractor in the phase space, the subset of allowed symbol sequences corresponds to a chaotic set em-

bedded in the attractor. As we will argue using a physical example, these sets are typically nonattracting chaotic saddles. We mention that making use of a chaotic saddle for communication has one practical advantage: It makes the message encoding immune to small noise (see Sec. II for details).

An issue of great importance in any digital communication scheme is how much information the system can encode and transmit. A quantitative measure of the amount of information is the *channel capacity* [3,4]. For a chaotic system, channel capacity is equivalent to the topological entropy [5] because this entropy defines the “amount” of information that can be transmitted through a communication channel [3,4]. From a dynamical point of view, the topological entropy measures the orbit complexity of the chaotic invariant set. From the viewpoint of information theory, the topological entropy is the rate at which information is generated. To give an example, consider again a string of n symbols generated by the dynamics. If the dynamics is purely random, one would expect to be able to observe 2^n possible symbol sequences. In this case, the topological entropy is simply

$$h_T = \lim_{n \rightarrow \infty} \frac{\ln 2^n}{n} = \ln 2,$$

which is the maximum possible value for processes defined by two symbols. A deterministic chaotic system is, however, not purely random. Thus, if the symbolic dynamics requires only two symbols, the topological entropy of the attractor is generally less than $\ln 2$ [6]. Since a coding scheme makes use of only an invariant subset embedded in the attractor, and since the topological entropy of the subset cannot be larger than that of the attractor, the channel capacity in any practical communication scheme employing a code must be less than or equal to that which would be produced in the ideal situation where the entire attractor is used for encoding messages.

The second result of the paper is detailed analyses and numerical confirmation for the topological entropies of a family of chaotic saddles embedded in a chaotic attractor. In particular, we argue that an appropriate code restriction exists that generates a noise-resisting chaotic saddle to optimize the tradeoff between the channel capacity and the noise resistance. Let the noise resistance be simply measured by the noise amplitude. We provide strong evidence that indicates that the topological entropy is a nonincreasing and devil’s-staircase-like function of the noise amplitude, a statement that can be made rigorous for some simple discrete chaotic maps. The plateau regions in the devil’s staircase indicate that the dynamical complexity of the chaotic saddle is structurally stable with respect to variations in the noise-resisting strength. The main practical implication of our result is that chaotic saddles embedded in a chaotic attractor can be naturally utilized as noise-resisting but rich information source for digital communication. A short account of this work has been reported in Ref. [7].

The rest of the paper is organized as follows. In Sec. II, we present a physical example with the Lorenz system to illustrate that a coding scheme generates a chaotic saddle in the phase space. In Sec. III, we present numerical results of the topological entropy for chaotic systems described by

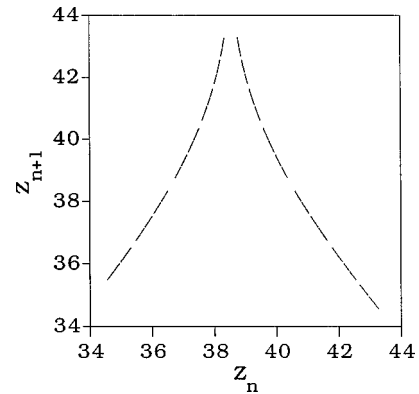


FIG. 1. A 10 000 point trajectory of the Lorenz map on a noise-resisting chaotic saddle embedded in the chaotic attractor, corresponding to imposing the grammatical restriction, “no four zeroes in a row.”

both one-dimensional noninvertible and two-dimensional invertible maps. In Sec. IV, we give a detailed theoretical analysis for the devil’s-staircase-like function of the topological entropy versus the noise amplitude. In Sec. V, we present a rigorous result for the topological entropy function of the chaotic saddles for the one-dimensional logistic map $f(x) = 4x(1-x)$. In Sec. VI, we construct, by making use of the classic middle-1/3 Cantor set, a simple phenomenological model that captures the essential behaviors of topologically varying the chaotic saddles embedded in a chaotic attractor. Using this model, the devil’s-staircase-like behavior of the topological entropy can be understood in a straightforward manner. In Sec. VII, we present discussions.

II. AN EXAMPLE OF CODING: THE LORENZ SYSTEM

We consider the Lorenz system [8]:

$$\begin{aligned} \dot{x} &= 10(y-x), \\ \dot{y} &= x(28-z) - y, \\ \dot{z} &= xy - (8/3)z. \end{aligned} \quad (1)$$

The Lorenz system has been a paradigm in the study of chaotic systems and it can in fact be physically realized by an electronic circuit [9]. Let z_n be the maxima of the state variable $z(t)$. Then, on the ω -limit set, the successive local maxima can be described by a one-dimensional map,

$$z_{n+1} = f(z_n). \quad (2)$$

The chaotic attractor in the phase space $\{x(t), y(t), z(t)\}$ corresponds to a one-dimensional chaotic attractor in the phase space of the discrete map $f(z)$. The natural partition for defining a good symbolic dynamics is the critical point z_c where $f(z_c)$ is maximum. A trajectory point with $z < z_c$ ($z > z_c$) bears the symbol $\mathbf{0}$ ($\mathbf{1}$). Now suppose we choose a code in which *four zeroes in a row is forbidden* in any n -bit sequence, where $n > 4$. In the symbolic space, the code removes an open set of symbols. In the phase space of the map $f(z)$, the restriction imposed by the code removes a gap around the cusplike maximum, and all of its preimages. There are an infinite number of preimages at all scales and,

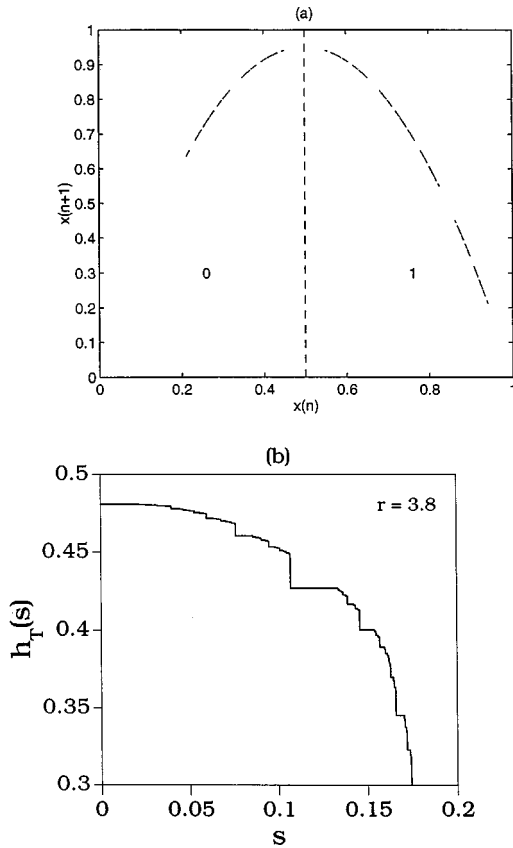


FIG. 2. (a) A trajectory of 50 000 points on a noise-resisting chaotic saddle of gap size $s=0.1$ embedded in the chaotic attractor of the logistic map $f(x)=3.8x(1-x)$. The trajectory is computed by using the PIM triple method. (b) The topological entropy h_T vs the noise-resisting gap size s for the logistic map at $r=3.8$.

less than or equal to that of the attractor. As the noise-resisting gap size s increases, h_T must not increase; i.e., h_T must decrease or remain constant. To address the tradeoff between the channel capacity and noise resistance of the chaotic saddle, we investigate the behavior of the topological entropy as the gap size s is systematically increased. Figure 2(b) shows $h_T(s)$ versus s , for fixed $r=3.8$. To compute $h_T(s)$ for each value of s , we count $N(n)$, the number of possible symbol sequences of length n that are allowed by trajectories on the corresponding chaotic saddle with the primary gap size s . The topological entropy is given by

$$h_T = \lim_{n \rightarrow \infty} \frac{\ln N(n)}{n}. \quad (4)$$

In practice, we approximate this limit by linear regression to a plot of $\ln N(n)$ versus n for n up to, say, 20; the slope of the plot is approximately the topological entropy h_T . In Fig. 2(b), we see that h_T is apparently a nonincreasing function of s . An interesting phenomenon is that there are regions of s in which h_T remains approximately constant. Numerically, we find that these plateau regions appear to exist on all scales in s . The set of s values at which h_T changes seems to have arbitrarily small Lebesgue measure in the parameter space of s . Similar behavior is observed for other parameter values of the logistic map, such as the one with well developed chaos, as shown in Fig. 3 for $r=4$. These numerical results thus

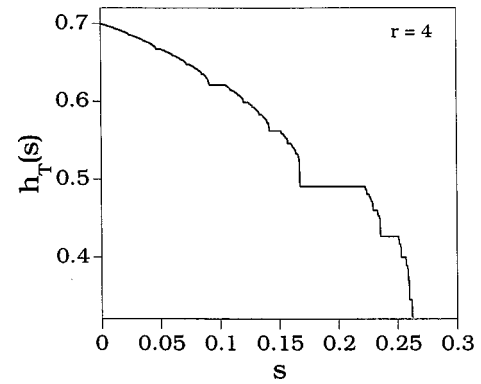


FIG. 3. Numerical computation of the topological entropy h_T vs the size of the noise-resisting gap s for the logistic map at $r=4$.

strongly suggest that the function of h_T versus s is a devil's staircase.

A feature of the h_T -versus- s function, which is common to chaotic parameter values of r [Figs. 2(b) and 3] and of *practical importance*, is that h_T decreases only slightly in a wide region when the noise-resisting gap size increases from zero initially. In Fig. 3, for example, the topological entropy of the chaotic attractor is $\ln 2 \approx 0.69$. As s is increased from 0 to 0.1, h_T decreases from $\ln 2$ to about 0.62, a rather small decrease. But $s=0.1$ means that the symbolic dynamics on the chaotic saddle is robust against noise of amplitude about 5×10^{-2} . Thus, with only incremental loss in the channel capacity, the symbolic dynamics on the chaotic saddle is immune to external noise of relatively large amplitude.

The result that the topological entropy of the noise-resisting chaotic saddles embedded in a chaotic attractor is a nonincreasing and devil's-staircase-like function of the noise-resisting gap size appears also to be true for chaotic systems described by two-dimensional maps. A main difficulty for maps of two dimensions and higher, however, is to identify a partition curve in phase space so that a good symbolic dynamics can be defined. Due to nonhyperbolicity [12] of chaotic attractors in typical two-dimensional maps, such a partition curve usually consists of line segments connecting all primary tangency points between stable and unstable manifolds [13]. It is thus a highly nontrivial task to construct symbolic dynamics in high dimensions. However, it can be argued that the utilization of chaotic saddles with noise resisting gaps tremendously simplifies the task of identifying partition curves. To illustrate this, we consider the Hénon map [14]

$$x_{n+1} = 1.4 - x_n^2 + 0.3y_n, \quad (5)$$

$$y_{n+1} = x_n,$$

for which it is believed to exhibit a chaotic attractor. For a trajectory on this attractor, the symbolic partition is a zigzag curve lying in the vicinity of the x axis, which connects all primary tangencies [13,15]. The dynamics on the attractor can thus be represented by that of two symbols in the symbolic space: points above (below) the partition curve correspond to a symbol **1** (**0**).

Now consider a chaotic saddle embedded in the attractor with a noise-resisting gap of size $s=0.25$ that covers the

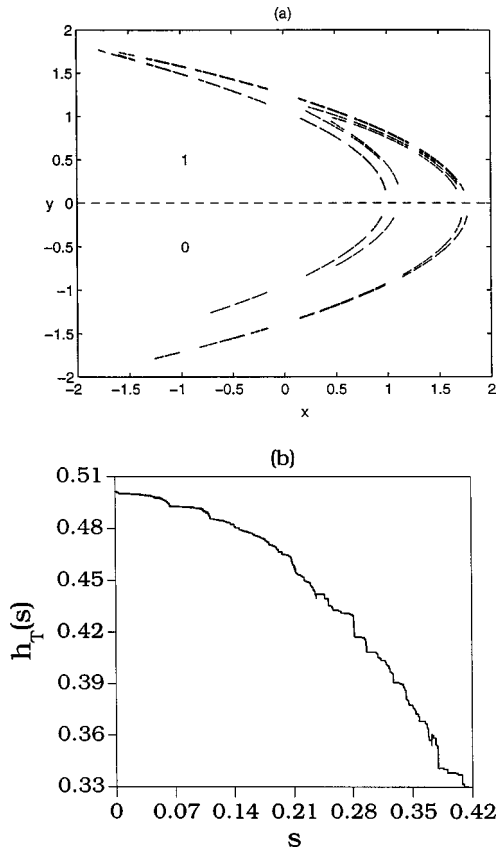


FIG. 4. (a) For the Hénon map, a noise-resisting chaotic saddle embedded in the chaotic attractor of gap size $s=0.25$. (b) The topological entropy h_T vs the noise-resisting gap size s for the Hénon map.

partition curve entirely, as shown in Fig. 4(a). For trajectories restricted to the chaotic saddle, specification of the partition is now straightforward: points with $y>0$ bear symbol **1**, and those with $y<0$ correspond to **0**. Chaotic saddles such as the one in Fig. 4(a) can be computed using the PIM triple method similar to that for one-dimensional maps [16]. Specifically, to generate Fig. 4(a), we have used 100 points on a random line segment in the square $-1 \leq (x,y) \leq 1$ to refine a PIM triple, and the size of the refined triple is 10^{-9} . Here, too, increasing the gap width decreases the measure of the chaotic saddle. Figure 4(b) shows h_T versus s for $0 \leq s < s_{\max} \approx 0.42$, where for each value of s , the topological entropy is computed by counting the number of possible two-symbol sequences of various lengths corresponding to trajectories on the chaotic saddle. Again, h_T versus s is a nonincreasing, devil's-staircase-like function. As s increases from 0, h_T decreases slowly at first, and then faster, which warrants a relatively large regime $s < s_c \approx 0.14$ within which h_T decreases only slightly.

Thus, utilizing chaotic saddles with noise-resisting gap size close to s_c seems to be practically beneficial in communication applications: (i) the specification of the symbolic dynamics is straightforward, (ii) the symbolic dynamics is robust even in a noisy environment, (iii) yet the channel capacity is close to that obtained when one utilizes the original chaotic attractor.

We emphasize that we utilize the PIM triple method only for the purpose of a systematic study of the tradeoff between

the channel capacity and the noise resistance of chaotic saddles. In practice, chaotic saddles with a noise gap embedded in a chaotic attractor can be easily generated even from an experimental data set by imposing an appropriate code restriction. Recall that the chaotic saddle of the Lorenz map, pictured in Fig. 1, was generated directly from (numerical) experimental data by eliminating four zeroes in a row from the grammar. In fact, a gap is effectively and automatically generated during the transmitting step, when communicating, simply by never transmitting a “gap grammar” sequence **0000**, for example, by incorporating “buffer” bits as appropriate. An analogous gap-grammar design is likely to work well with 2D symbolic dynamics by appropriately restricting the so-called “pruning front” [15].

IV. THEORY

We now present a detailed theoretical justification for the devil's staircase of the h_T versus noise-resistance gap function seen in numerical experiments. At present our theory applies only to one-dimensional and one-hump maps such as the logistic map or the Lorenz map. Briefly, the idea is as follows. We study a sequence of successive approximations to the grammar of the symbolic dynamics as the length of the symbol sequences (words) increases. The dynamics in the symbolic space can then be represented by a sequence of transition matrices characterizing all the possible, or forbidden, transitions between words. The topological entropy associated with the symbolic dynamics can then be obtained by considering the limit of the spectral properties of the transition matrices.

A. Computation of topological entropy by transition matrices

Without loss of generality, we consider one-dimensional and one-hump maps defined on the unit interval $M \equiv [0,1]$. For such a map, there is a critical point $0 < x_c < 1$. This critical point is often chosen to be the generating partition and, hence, we have $S_0 = [0, x_c]$, $S_1 = (x_c, 1]$. A trajectory point x bears a symbol **0** if $x \in S_0$ and a symbol **1** if $x \in S_1$. An initial condition then has an itinerary sequence $\sigma = \sigma_0 \sigma_1 \sigma_2 \sigma_3 \dots$, where $\sigma \in \Sigma$, and Σ represents the symbolic space that consists of all possible infinite symbol sequences of the symbols **0** and **1**. Since the chaotic dynamics of $f(x)$ is deterministic, typically, only a subset of all possible symbol sequences can be generated by a typical chaotic trajectory. Denote the symbolic subspace in which we find the symbolic itineraries of all trajectories of a given invariant chaotic set by $\Sigma' \subset \Sigma$. The action of the map in the phase space then corresponds to the following Bernoulli-shift map in the subspace Σ' ,

$$s(\sigma) = s(\sigma_0 \sigma_1 \sigma_2 \sigma_3 \dots) = \sigma_1 \sigma_2 \sigma_3 \sigma_4 \dots \quad (6)$$

By construction, the dynamics in the subspace Σ' is invariant in the sense that if $\sigma \in \Sigma'$ then $s(\sigma) \in \Sigma'$. The subspace Σ' is called a *subshift* (the full space Σ is called the *full shift*) [17].

A subshift of finite type has a grammar that can be represented by a finite list of forbidden n -bit words. In this case, the grammar can be described by a 2^n -node directed graph, or equivalently, by a $2^n \times 2^n$ transition matrix, A_n , as shown

in Fig. 5(a) for $n=4$. The Bernoulli-shift map permits at most two arrows into and two arrows out of each n -bit node, corresponding to the choice of shifting in a $\mathbf{0}$ or a $\mathbf{1}$ into the least significant bit from any state. For a full-shift grammar, there are no forbidden n -bit words and, hence, each row and each column of the transition matrix A_n has *exactly* two non-zero entries. For a subshift grammar, each row and each column of A_n has *at most* two nonzero entries, because there are now forbidden words. The grammar of the subshift, or the symbolic dynamics, is completely specified by A_n in the limit $n \rightarrow \infty$.

By conjugacy of $s|_{\Sigma'}$ to $f|_M$, the topological entropy of the two dynamical systems is the same,

$$h_T(\Sigma') = h_T(M). \quad (7)$$

The topological entropy of a subshift of finite type can be computed directly as the natural logarithm of the spectral radius of the generating transition matrix [17],

$$h_T(\Sigma'_{A_i}) = \ln[\rho(A_i)]. \quad (8)$$

The topological entropy of a subshift of infinite type can be computed in terms of the limit of spectral radii of a sequence of transition matrices $\{A_i\}$, which generate a sequence of subshifts $\{\Sigma'_{A_i}\}$ to Σ' of increasing accuracy,

$$h_T(\Sigma') = \lim_{i \rightarrow \infty} \ln[\rho(A_i)]. \quad (9)$$

We require the spectral radii of a sequence of thousands of matrices, each of which is $2^m \times 2^m$ and we choose $m = 14$. Obviously, finding the roots of thousands of mammoth characteristic polynomials is impractical. Numerically, we compute the spectral radius of a given matrix B , by a slight modification of the power method. The power method relies on the fact that upon iteration, almost all initial vectors are rotated towards the dominant eigenspace (the subspace corresponding to the largest eigenvalue). In the case of a Perron-Frobenius operator, the dominant eigenvalue is guaranteed to be a simple root, and the dominant eigenspace is one dimensional. Given an arbitrary initial unit vector \mathbf{u}_0 , and the iteration scheme, $v_n = B u_{n-1}$, with normalization during each step, $u_n = v_n / \sqrt{v_n^T v_n}$, it can be shown that as $n \rightarrow \infty$, $\sqrt{v_n^T v_n} \rightarrow \lambda_0$, the dominant eigenvalue. The proof is quite simple [19], beginning with the observation that an arbitrary vector \mathbf{u}_0 can be written as a linear combination of the eigenvectors of B , and that if $|\lambda_0| > |\lambda_i|$, then $|\lambda_0|^n$ dominates $|\lambda_i|^n$, for large n . Our matrices are so large that even the straightforward application of the power method, which is simply iterative matrix multiplication, is too costly, as even a single matrix multiplication $B u_n$ of a $2^{14} \times 2^{14}$ matrix requires 2^{28} addition and multiplication steps. However, we avoid this problem by noting the particularly sparse structure of our subshift generating matrices. Each row and each column of our matrices has at most two nonzero entries, corresponding to the possibility of shifting in either a zero or a one bit from each node (n -bit word). With this consideration, a matrix multiplication routine can be tailored to multiply our $2^{14} \times 2^{14}$ matrix by a vector using only 2^{15} multiplications and additions.

Let $M(s)$ denote the chaotic saddle, embedded in the chaotic attractor of $f(x)$, with a primary noise-resisting gap of size s centered at the critical point x_c . If we know the form of the subshift $M(s)$, we can make use of Eq. (9) to compute $h_T[M(s)]$, the topological entropy of the chaotic saddle. In principle, this technique can be extended to high-dimensional maps.

B. Restricting the grammar: topological entropy of the chaotic saddle

Given a one-hump map, such as the logistic map, the key feature that allows us to apply Eq. (9) to calculate the gradually varying topological entropy, as a function of gap size s , is the fact that we know the order of the n -bit itinerary bins, along the unit interval. Due to continual refolding of the interval back into itself, the order of itineraries of a one-hump map is not given directly from the norm of its symbol code, $\|\sigma\|$, but is found by an alternating binary tree (see, for example, Fig. 2 of Ref. [15]), which generates an order called the *unimodal order* [20,21]. For example, the 2-bit words in the increasing unimodal order are $00 < 01 < 11 < 10$.

When formulating an n -bit word approximation of the subshift Σ' , we construct the $2^n \times 2^n$ transition matrices ordered according to the unimodal order. For each n -bit approximation of the full shift grammar (no word restrictions), each of the 2^n nodes has two entering arrows and two exiting arrows. Therefore the transition matrix A_n has exactly two ones in each row and column, and it follows that $h_T(A_n) = \ln[\rho(A_n)] = \ln(2)$. A restriction on the grammar of Σ'_{A_n} corresponds to a forbidden n -bit word. If the j th n -bit word is forbidden, then all transitions into and out of the j th node are also forbidden so that the invariance of the subshift with respect to the Bernoulli-shift map is preserved. Hence, the corresponding transition matrix A'_n has all zero entries in the j th row and the j th column.

We now analyze how the topological entropy of the chaotic saddle changes as the size of the noise-resisting gap s increases. For illustrative purposes we study the logistic map at $r=4$. In this case, for the chaotic attractor the symbolic dynamics is (almost [18]) a full shift. Thus, transitions between (almost) all words are allowed. Figure 5(a) shows all the possible transitions among all 4-bit words, together with the transition matrix A_4 . When $s=0$, no bins on the unit interval are forbidden, and therefore, no words are forbidden. We obtain

$$h_T(s=0) = h_T(A_4) = \ln(2). \quad (10)$$

As s increases (symmetrically about $x_c=0.5$), there is no effect to the 4-bit grammar approximation until the bins labeled 0.100 and 1.100 are eliminated, at a critical value s_{cr_1} when the gap radius is exactly the width of these bins. Removing these bins from the chaotic attractor M implies that the itineraries 0.100 and 1.100 will never occur in the corresponding subshift. Therefore, we restrict (i.e., reduce by adding more rules) the grammar of Σ'_{A_4} to the smaller subshift $\Sigma'_{A'_4}$, generated by A'_4 , by placing zeroes in the eighth and ninth rows and columns of A_4 , as shown in Fig. 5(b). By direct computation, we obtain

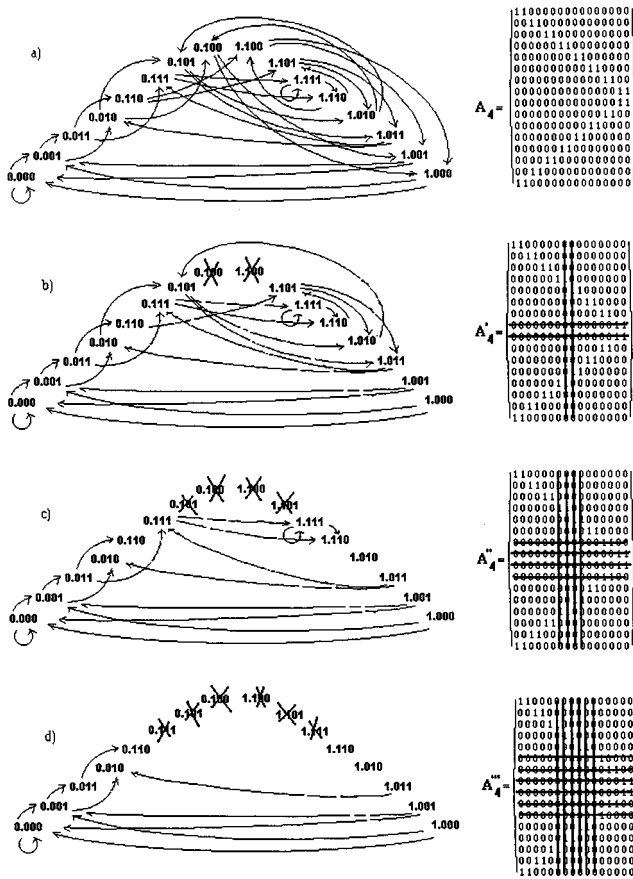


FIG. 5. For the logistic map at $r=4$, directed graph and the corresponding transition-matrix representations of subshifts of finite type generated by a 4-bit grammar. The $2^4=16$, 4-bit words are arranged in increasing unimodal order, left to right, just as they occur in one-hump maps, $0.000 < 0.0001 < 0.011 < \dots < 1.001 < 1.000$. The nodes (words) are further arranged in a manner to suggest a one-hump map. (a) The full shift grammar as generated by A_4 . Each node has two arrows in, and two arrows out, corresponding to unrestricted possibility of shifting in a 0 or a 1 bit at all bins. The 16×16 transition matrix A_4 has two ones in each row (each node has two possible outcomes) and two ones in each column (each node has two possible preimages), where $A_{i,j}=1$ denotes an arrow from the i th node to the j th node. By ordering state vectors according to the unimodal code, and hence also the transition matrix, we see the ones in the transition matrix form a “V” on its side, suggesting the one-hump map whose dynamics is represented. (b) The gap s is widened to the critical value s_{cr_1} , which exactly eliminates the bins 0.100 and 1.100 in the logistic map. The corresponding nodes (the 8th and 9th) must also be eliminated, as well as arrows in and out of these two nodes. Likewise, the transition matrix A'_4 has zeroes in the 8th and 9th rows and columns. Nodes eliminated are covered by an “ \times ,” but other nodes are also effectively eliminated. These nodes have no entering arrows, and hence are never visited. A'_4 generates the subshift $\Sigma_{A'_4}$. (c) When the gap is further widened to the critical discrete value $s=s_{cr_2}$, a 4-bit change in the subshift occurs. (d) When $s=s_{cr_3}$, the channel capacity of the directed graph collapses. No circuits through the graph, which have two arrows out of a node, remain.

$$h_T(s=s_{cr_1}) = h_T(A'_4) = \ln[\rho(A'_4)] = \ln\left(\frac{1+\sqrt{5}}{2}\right). \quad (11)$$

As s continues to increase, there is no effect to the 4-bit

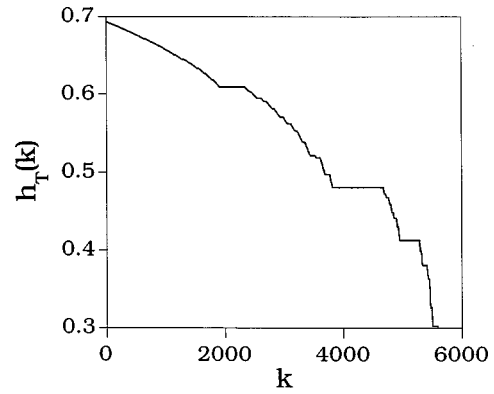


FIG. 6. Topological entropy h_T vs the noise-resisting gap k . This calculation is based on a Markov model of the grammar of a subshift of finite type, where k is the number of n -bit forbidden words, and $n=14$. The topological entropy is calculated directly from the logarithm of the spectral radius of the evolving transition matrices $A_n^{(k)}$. We begin with the n -bit representation of the full shift grammar. The plot is qualitatively similar to that in Fig. 3.

grammar approximation until s reaches a second critical value s_{cr_2} when the itineraries 0.101 and 1.101 must also be forbidden from the new subshift $\Sigma_{A''_4}$, as shown in Fig. 5(c). The topological entropy thus decreases again at s_{cr_2} . As s increases further passing another critical value, the itineraries 0.111 and 1.111 are eliminated, as shown in Fig. 5(d). This causes a new decrease in the topological entropy.

Although, in general, we do not know a priori the locations and widths of each n -bit itinerary bin in the case of one-dimensional maps, we do know the order in which they are eliminated: this follows the unimodal code order for one-hump maps. (In fact, we can find the critical gap widths for the logistic map for $r=4$ by using the invariant measure $\mu(x) = (1/\pi)[x(1-x)]^{-1/2}$ [22]). To compute the function $h_T(s)$ in a systematic way, we start with the full shift grammar Σ_{A_n} , where A_n is ordered according to the occurrence of n -bit itineraries on the unit interval, and then eliminate pairs of n -bit words (by zeroing corresponding rows and columns), starting from the middle, to simulate the effect of widening the gap size s centered at $x_c=1/2$. At each step, we compute $h_T(k)$, where k is the number of n -bit forbidden words, of the evolving subshift, directly from the spectral radius of the current transition matrix $A_n^{(k)}$ in which $2k$ words are eliminated. Figure 6 shows $h_T(k)$, where k scales monotonically with the gap width s and, at each value of k , $2k$ bins are eliminated from the grammar. We see that the topological entropy appears to be a nonincreasing function of k . Increasing n , the word size considered, better approximates the effect of continuously increasing the gap size s from $s=0$ and, hence, more structure in the function $h_T(k)$ can be resolved.

C. The devil’s staircase entropy function

The structure of the function $h_T(k)$ in Fig. 6 resembles that of a devil’s staircase. As n is increased, more constant intervals, or “flat spots,” are revealed. The reason for these flat spots is that the topology of the chaotic saddle $M(s)$ does not change for an interval of values of the gap size s .

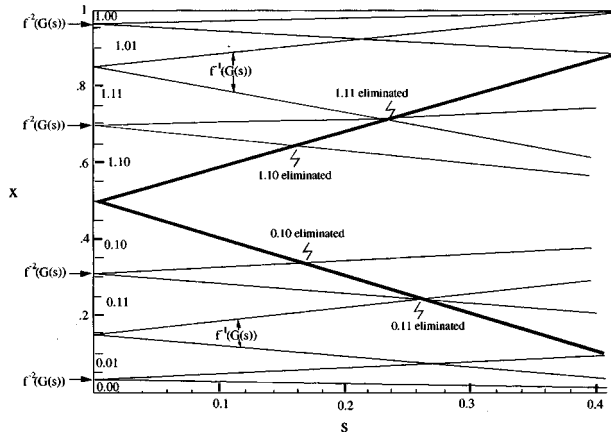


FIG. 7. The “tonguelike” gaps $G(s)$ (bold boundary) and preimages $f^{-i}(G(s))$ of the logistic map $f(x) = 4x(1-x)$. Note that as the gap width s increases, the n -bit word bins decrease. Due to nonuniformly distributed tongue “centers” and varying rates of tongue contraction, words are eliminated for varying values of s . This picture is seen on all scales, for increasing n .

For the logistic map at $f_4(x) = 4x(1-x)$, it is possible to prove, by geometric argument, that the function $h_T(k)$ is indeed a devil’s staircase, which we will do in the following.

We first consider the case $s = 0$. All the n -bit symbol sequences are distributed in the unit interval in various bins, the boundaries of which are generated by the preimages of the critical point $c \equiv 1/2$ (the partition), $\{x_c, f_4^{-1}(x_c), \dots, f_4^{-(n-1)}(x_c)\}$. Since there are 2^{n-1} branches of $f_4^{-(n-1)}(x_c)$, there are $\sum_{i=1}^n 2^{i-1} = 2^n - 1$ total preimages, including the partition itself. For $r = 4$, these preimages are all in the unit interval and they are dense as $n \rightarrow \infty$. It should be noted that the logistic map f_4 is semiconjugate to the full shift. However, the lack of a full conjugacy is not serious in this case because it is only due to the ambiguity of assigning itineraries to set of preimages of x_c : $\cup_{i=0}^{\infty} f_4^{-i}(x_c)$ [18]. We can treat the equivalence as if it were a conjugacy with respect to the issue of topological entropy.

Next we consider increasing the gap width s . Let $M(0) = [0, 1]$ denote the full attractor at $s = 0$, and let

$$M(s) = [0, 1] - \cup_{i=0}^{\infty} f_4^{-i}[(\frac{1}{2} - s, \frac{1}{2} + s)] \quad \text{for } s > 0 \quad (12)$$

denote the chaotic saddle when $s \neq 0$. The saddle is a Cantor set that consists of the original attractor excluding the noise-resisting gap and all its preimages. In general, there are overlaps between preimages of the primary gap $G(s) \equiv (1/2 - s, 1/2 + s)$.

Qualitatively, the amount of overlap changes as s changes in such a way that the topological entropy $h_T(s)$, as a function of s , is characterized by a devil’s staircase. To see this, we plot the primary gap, and a few preimages for varying size s , as shown in Fig. 7, where the two bold lines define the primary gap:

$$x = \frac{1}{2} = s \quad \text{and} \quad x = \frac{1}{2} - s. \quad (13)$$

The curves that define the first preimage of the primary gap are given by

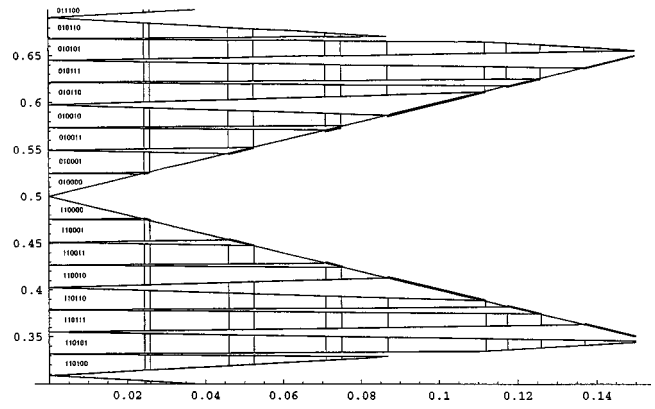


FIG. 8. A blowup inset of Fig. 7, with an increased grammatical precision of $n = 6$ bit words and tonguelike gaps through $f_4^{-m}(G(s))$, where $m = 0, 1, 2, 3, 4, 5$. Vertical line segments cut through the tongues marking critical values $s_{cr} = a$ when a $f_4^{-i}(G(s))$, for some $i = 0, 1, \dots, 5$, first intersects the main gap $G(s)$, thus beginning an interval $s \in (a, b)$ in which the chaotic saddle $M(s)$ does not change topologically, despite increasing s . The topological entropy $h_T(s)$ is therefore constant for $s \in (a, b)$.

$$f_{4,\pm}^{-1}(x) = \frac{1 \pm \sqrt{1-x}}{2}. \quad (14)$$

There are four such curves, as shown in Fig. 7. This figure can be considered a bifurcation diagram of the gaps, or word bounds, in the parameter s . The second preimage of the primary gap consists of four smaller gaps bounded by eight curves $f_{4,\pm}^{-2}(G(s))$, as shown in Fig. 7. Considering all these gaps, we see a total of up to seven gaps (exactly seven before gaps collide), and eight symbol bins. Note that the successive preimages of the primary gap form successively tighter tonguelike structures. These tongues occur on all scales, accounting for all preimages of the primary gap.

Geometrically, the tongues in Fig. 7 correspond to the gaps $f_4^{-m}(G(s))$ that bound the symbol bins. As s is increased from zero, the space in between the two tongues is eliminated. Whenever the two tongues intersect, the originally allowed words that lived in the space becomes forbidden. That is, whenever the following occurs,

$$f_4^{-m}(G(s)) \cap f_4^{-n}(G(s)) \neq \emptyset \quad \text{for any } m, n > 0, \quad (15)$$

some words are eliminated. Due to the varying tightness of the tongues, for different pre-images of the main tongue $G(s)$, the overlap among them occurs at different values of s . For instance, in Fig. 7, we see that 0.10 and 1.10 are eliminated at a smaller gap width s than the value of s at which 0.11 and 1.11 are eliminated.

The above consideration thus leads to the following theorem:

Theorem: Given the logistic map $f_4(x) = 4x(1-x)$, the topological entropy function $h_T(s)$ is constant on the complement of a Cantor set of s values.

The proof of the theorem is sketched as follows. Consider Fig. 8, a blowup of part of Fig. 7 in the narrowed range $x \in [0.3, 0.7]$, where we have increased the precision of the grammatical representation to $n = 6$ bit words by showing

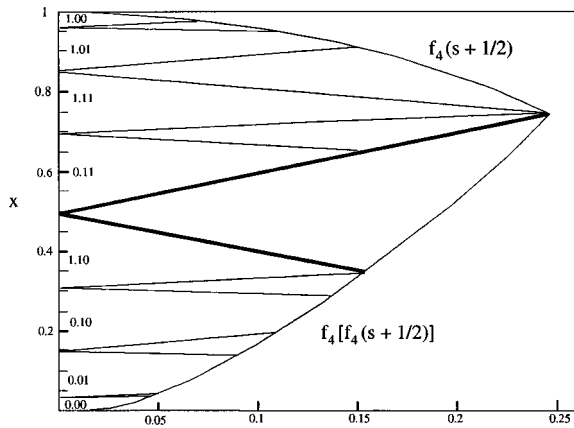


FIG. 9. The chaotic saddle $M(s)$ as a function of s . $M(s)$ is contained between the two curves, $f_4(s + \frac{1}{2})$ and $f_4(f_4(s + \frac{1}{2}))$, the first two iterates of the main gap $G(s)$, but these are not sharp bounds, due to ‘‘tongue’’ (word) overlap. Parameter values $s = a$ when 3-bit words first overlap, are marked.

the gaps $f_4^{-m}(G(s))$ for $m = 0, 1, 2, 3, 4, 5$. Consider a vertical line segment of constant s , say,

$$s = 0.01, \quad 0 \leq x \leq 1. \tag{16}$$

Such a line cuts through the countably infinite number of tongues: there is one $G(s)$, and two $f_4^{-1}(G(s))$, and four $f_4^{-2}(G(s))$, ..., and 2^m of $f_4^{-m}(G(s))$, etc. Thus, we remove the open intersections between the gaps and the line segment, leaving a Cantor set in the phase space x . As the value of s is increased, some tongues intersect, and therefore they overlap as s is increased further, eliminating branches of the Cantor set. At the critical value bounded by $s \leq 0.25$, the Cantor set no longer exists, as shown in Fig. 9.

The topology of increasing the noise-resisting gap is similar to the construction of the fixed $s = 0.01$ Cantor set described in the previous paragraph, but for variable gap widths, the set of intersection with the tongues is the line segments,

$$s = x - \frac{1}{2} \quad \text{and} \quad s = \frac{1}{2} - x, \quad \text{where} \quad 0 \leq s \leq 1. \tag{17}$$

These two line segments intersect the tongues at various values of s , and therefore at various opening widths of the tongues. For small s , all tongues $f_4^{-m}(G(s))$ are intersected when they are narrow, and for larger s , tongues are intersected in a wider state. Removing the open intersection between the tongues, and the line segments of Eq. (17) leaves a Cantor set, which we call C_{tongue} , but whose measure is not uniformly distributed, by construction. The projection of C_{tongue} onto the s axis is also a Cantor set, due to monotonicity of Eq. (17). We call this set C_s .

As s is increased through a tongue, the chaotic saddle $M(s)$ is unchanged, as such a change in s essentially just increases the overlap between the main gap $G(s)$, and an ‘‘already removed’’ preimage $f_4^{-m}(G(s))$. An m -bit word is eliminated at exactly the value of s when $G(s) \cap f_4^{-m}(G(s))$ is first nonempty, for each given branch cut of $f_4^{-m}(G(s))$, for each $m > 0$. Therefore, the topology of the set $M(s)$ does not change on the complement of the Cantor set $s \in \bar{C}_s$, and

the topological entropy $h_T(s)$ of $f_4|_{M(s)}$ is constant when the topology of $M(s)$ is constant. A function that is constant in the gaps of a Cantor set, and therefore may only change on the Cantor set, is a devil’s staircase function.

Note that we have not shown that the topological entropy actually does change for s in the Cantor set C_s , only that it does not change in the Cantor gaps. We claim that, at least in the case of the logistic map $f_4|_{M(s)}$, the topological entropy does in fact change whenever the topology of $M(s)$ changes. Since each $x \in M(s) \subset [0, 1]$ has a unique symbolic code, the right-hand end point $R = \max\{z \in M(s)\}$ has the symbolic code $\sigma_R = h(R)$ that bounds all symbol sequences in the subshift of the chaotic saddle, $\sigma \in \Sigma'_{f_4|_{M(s)}}$ according to

$$\sigma \leq \sigma_R \tag{18}$$

where \leq is the unimodal order on the symbolic space [23]. Note that σ_R is the kneading sequence of the one-dimensional map [24]. Any loss of points in $M(s)$ that causes a loss of words in the corresponding subshift leads to a decrease in the topological entropy that measures the asymptotic growth rate of the word count of n -bit words. This argument does not apply to restricting a map of the interval for which we cannot make the statement that each point has a unique symbolic code, as, for example, in the case of maps with constant regions, or maps with attracting periodic orbits.

Corollary: The symbolic dynamics of $M(s)$ are of finite type, for s supported on the complement of a Cantor set.

Therefore, the complex case of a grammar of infinite type can only be supported on the Cantor set. Furthermore, there is a structural stability associated with each resulting grammar of finite type, as manifested by the flat spots of constant topology; i.e., a given complexity is persistent.

It is insightful to plot the $n = 3$ approximation of $M(s)$ as a function of s , as shown in Fig. 9. The chaotic saddle $M(s)$ is contained between the two curves,

$$f_4(s + \frac{1}{2}) \quad \text{and} \quad f_4(f_4(s + \frac{1}{2})). \tag{19}$$

These are the first two iterates for the boundary of the main gap $G(s)$, which act as the envelope bounding $M(s)$; they are only bounding envelopes because as each of the curves passes through a tongue, the set $M(s)$ is unchanged. This is just another way of viewing exactly the same argument of tongue overlap as a function of s , described in previous paragraphs.

There is a question as to whether the tongues overlap so much as to cause an empty set C_{tongue} . This depends on the placement of the tongues, and whether preiterates of tongues shrink fast enough to prevent overlap everywhere. Thus, our argument applies to situations where some overlap with increasing s is allowed. In the next section, we investigate the distribution of measure along these Cantor sets, using a ‘‘tongues model’’ based on the ‘‘middle-1/3’’ Cantor set, thus explaining a feature in the graph of $h_T(s)$ with practical importance: the initially shallow decline of $h_T(s)$ is followed by the precipitous decrease of the channel capacity.

V. A PHENOMENOLOGICAL MODEL FOR THE ENTROPY FUNCTION

In this section, we develop a model, based on the middle-1/3 Cantor set, with a similar topology of ‘‘tongues’’ as that displayed by the noise-resisting chaotic saddles $M(s)$. The model helps to explain a feature in the graph of $h_T(s)$ that has particular practical importance: the initially shallow decline of $h_T(s)$ is followed by a precipitous collapse of the channel capacity. We also argue that the Cantor set C_{tongue} tends to be a multifractal whose measure distribution is concentrated near $s=0$ and falls off with increasing s .

The classic middle-1/3 Cantor set $C_{1/3}$ is the closed subset of the unit interval $[0,1]$, which is the limit of the sequence, $J_0=[0,1]$, $J_1=J_0-(1/3,2/3)$, $J_2=J_1-(1/9,2/9)-(7/9,8/9), \dots$, and J_n is the union of 2^n pairwise disjoint closed intervals of length 3^{-n} , and

$$C_{1/3} = \bigcap_{i=0}^{\infty} J_i. \tag{20}$$

Before we construct the set of tongues, it is useful to write the centers of each removed gap; of each J_i , in a closed form. We use a ternary expansion, which is analogous to the usual decimal expansion. Any number x in the unit interval can be written in ternary form,

$$x = \sum_{i=0}^{\infty} \frac{a_i}{3^i}, \quad a_i = 0, 1, \text{ or } 2. \tag{21}$$

A convenient characterization of $C_{1/3}$ is the set of all points whose ternary expansion contains no $a_i=1$, since $a_i=1$ signifies a point in a gap removed as part of J_i [25]. The center of the gap of J_1 is $c_1^{(1)}=1/2$, and the two new gaps' centers of J_2 are $c_2^{(1)}=1/6$ and $c_2^{(2)}=5/6$, which have the ternary expansions

$$\begin{aligned} \frac{1}{2} &= \frac{1}{3} + \frac{1}{9} + \frac{1}{27} + \dots = \overline{0.111}, \\ \frac{1}{6} &= \frac{1}{2} - \frac{1}{3} = \frac{0}{3} + \frac{1}{9} + \frac{1}{27} + \dots = \overline{0.0111}, \\ \frac{5}{6} &= \frac{1}{2} + \frac{1}{3} = \frac{2}{3} + \frac{1}{9} + \frac{1}{27} + \dots = \overline{0.2111}. \end{aligned} \tag{22}$$

We write the general form for a center $c_n^{(i)}$,

$$c_n^{(i)} = 0.b_1 b_2 \dots b_{n-1} \overline{111}, \quad b_i = 0 \text{ or } 2, \quad i = 1, 2, \dots, 2^{n-1}, \tag{23}$$

which lists the 2^n centers of J_n gaps.

In order to mimic the dynamic effect of widening the primary gap of the chaotic saddle, we consider a unit square in the two-dimensional plane, as shown in Fig. 10. We place the middle-1/3 Cantor set along the horizontal direction at $y=1$. As y decreases, we linearly decrease the gaps of the Cantor set to zero at $y=0$. Hence, although the Cantor at $y=1$ is middle 1/3, it is not middle 1/3 for $y \neq 1$. The set at $y=0$ is in fact not Cantor-like. Figure 10 is thus qualitatively similar to Fig. 7 in that the parameter y in Fig. 10 is equiva-

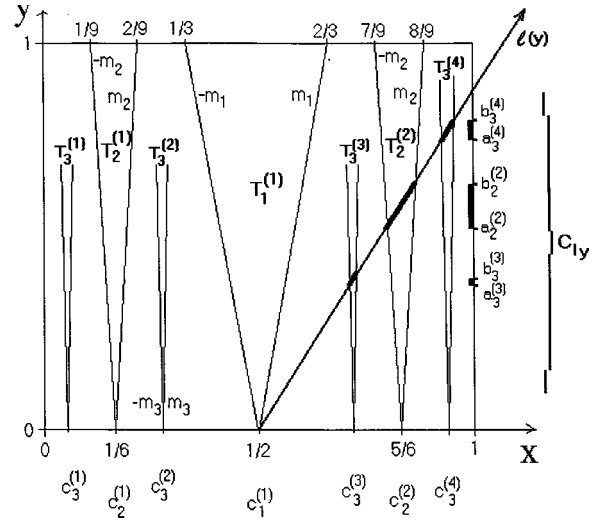


FIG. 10. A model of the tongues, based on scaling the middle-1/3 Cantor set. The line $l(y)$ intersects tongues of various widths, which depends both on height y , and on the level of the tongue in question. This determines the width of flat spots of the devil's staircase, the cumulative measure function $g(y)$ in Fig. 11.

lent to s in Fig. 7. There is an infinite number of tongues starting at $y=0$. Specifically, the lines

$$L_{n\pm}(y) = \pm \frac{y}{m_n} + c_n, \tag{24}$$

where $m_n = 2 \cdot 3^n$, are right (+) or left (-) edges of a tongue. This equation follows immediately from Eq. (23) and the slope comes from the definition of an end point of J_n . Note that there is such a tongue for each branch of c_n , and we define a tongue T_n as the open interior between $L_{n-}(y)$ and $L_{n+}(y)$, for a fixed center c_n . So we see that for any fixed $y \in (0,1]$, a Cantor set is defined as

$$C(y) = [0,1] - G(y), \tag{25}$$

where

$$G(y) = \bigcup_{n=1}^{\infty} (L_{n-}(y), L_{n+}(y)), \tag{26}$$

whose measure is

$$m(C(y)) = 1 - \sum_{i=0}^{\infty} \frac{y}{3} \left(\frac{2}{3}\right)^i = 1 - y, \tag{27}$$

and we note that corresponding to each n , there are 2^{n-1} gaps. The measure is independent of the location of the intersections between the line $y = \text{const}$ and the tongue boundaries $L_{n\pm}(y)$. For $y > 1$, $C(y) = \emptyset$, since all of the gaps overlap simultaneously, and the Cantor set evaporates.

We can now investigate the intersection between the gaps and an arbitrary straight line. For example, the line

$$x = l(y) = \frac{y}{r} + \frac{1}{2} \tag{28}$$

starts at the main gap center $c_1 = 1/2$, but with a slope other than $1/r = m_1 = 6$, that of the main gap boundary $L_1(y)$. We

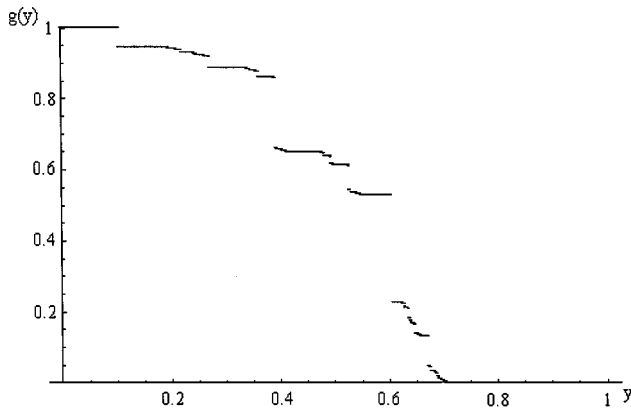


FIG. 11. The cumulative measure function $g(y)$ due to intersecting $l(y)$ with the scaled middle-1/3 Cantor set model of the tongues.

choose the line defined by, say, $1/r=7/4$, as pictured in Fig. 10, which intersects the tongues in a manner similar to the situation of widening a noise-resisting gap $M(s)$, described in previous sections, but here we can perform many of the calculations in closed form.

Intersections between lines $L_{n\pm}(y)$ and the line $l(y)$ can be found directly from Eqs. (24) and (28),

$$y = \left(\frac{c_n - 1/r}{\frac{1}{2} \mp 1/m_n} \right), \quad n > 1. \quad (29)$$

The intersection between $l(y)$, for $0 \leq y \leq 1$, and the tongues leaves a Cantor set, which we label C_l ,

$$C_l = \{l(y) : 0 \leq y \leq 1\} - \{l(y) : 0 \leq y \leq 1\} \cap (\cup_{n=0}^{\infty} T_n), \quad (30)$$

and we label C_{l_y} to be the projection of C_l onto the y axis. See Fig. 10.

Any positive monotone increasing function $f(y)$, restricted to C_{l_y} , will create a devil's staircase function with a profile similar to those seen in Figs. 2(b) and 3. We choose such a function: the measure of $C_{l_y} \cap [0, y]$ for example. Let

$$f(y) = m(C_{l_y} \cap [0, y]) = y - \sum_{n=2}^{\infty} \sum_{\substack{i=1 \\ y \leq a_n^{(i)}, b_n^{(i)}}}^{2^{n-2}} (b_n^{(i)} - a_n^{(i)}), \quad (31)$$

where $y = a_n^{(i)}$ and $y = b_n^{(i)}$ are the left and right end points of intersection between the tongue labeled $T_n^{(i)}$ and $l(y)$ according to Eq. (29). Since there are 2^{n-1} tongues $T_n^{(i)}$, or 2^{n-2} tongues to the right of $x=1/2$, there are up to 2^{n-2} tongues such that $y \leq b_n^{(i)}$. We calculate the devil staircase function,

$$g(y) = 1 - \frac{f(y)}{2}, \quad (32)$$

as shown in Fig. 11, by direct application of Eq. (31) (using a truncation of the infinite sum), in conjunction with the $c_n^{(i)}$ from Eq. (23).

Inspection of Fig. 10 reveals the explanation for the profile of $g(y)$. There are two factors regarding the behavior of $g(y)$. (1) If y is small, then the width of tongues $T_n^{(i)}$ tends to be in a narrower state when they intersect $l(y)$; and (2) for any given y , tongues $T_n^{(i)}$ are narrower than $T_{n-1}^{(i)}$, since $m_{n-1} < m_n$ (analogous to hyperolicity) and, hence, the gaps removed for large y are large, causing a precipitous decrease of $g(y)$. In other words, the Cantor set C_{l_y} has its cumulative measure density $f(y)$ weighted more heavily towards large y and it is a multifractal. Geometrically, the situation is analogous to considering the profile of the topological entropy versus noise-resisting gap as in Sec. IV C. The main difference is the way in which the tongues overlap: for this model, the T_n all overlap simultaneously when $y > 1$, which is in contrast to Sec. IV C, where the first overlap of tongues occurs for countably many different critical gap values s_{cr} .

The geometry extends to higher dimensions. In two or more dimensions, like coded n -bit regions define neighborhoods, or symbol bins, outlined by segments of (pre)iterates of the symbol partition curve. Widening a gap around the symbol partition curve propagates to the iterates of the partition, thus restricting the like-coded n -bit regions in a manner analogous to the tongues in one dimension. Given a two-dimensional map, for example, a bifurcation diagram graphing the phase space over a gap axis s could be used to depict three-dimensional conelike symbol tongues, each of which pinches off at a critical gap width. The middle-1/3 Cantor set model of this section generalizes to a Serinpinski carpet whose measure can be controlled by a parameter such as y .

VI. DISCUSSION

The basic principle that makes nonlinear digital communication with chaos possible lies in the fundamental link between chaos and information. The evolution of a chaotic system is unpredictable in the long term. In communication, a sequence of events conveys information if the events are not fully predictable (Shannon's point of view of information [3,4]). Thus, the fundamental unpredictability of chaotic systems implies that they can be regarded as sources that naturally generate digital communication signals. By manipulating a chaotic system in an intelligent way, useful information can be communicated [1].

A fundamental issue in communicating with chaos, as is in any digital communication scheme, is to select a code so that any message can be encoded into the signal to be transmitted. For chaotic systems, this is intriguing because, in general, there are grammatical restrictions imposed by the natural dynamics of the system. Designing a code that makes the best use of all the naturally occurring words is thus of paramount importance in order to realize communication. The results of this paper provide strong evidence that such an optimal code indeed exists for low-dimensional chaotic systems in general. We investigate the dynamics of coding and show that a practical coding scheme in communicating with chaos usually involves the utilization of chaotic saddles embedded in a chaotic attractor. This, in fact, has the advantage of strong noise resistance, but with only insignificant loss of

the channel capacity. To better see this, imagine that the topological entropy of the chaotic saddle decreases only slightly in a range of gap sizes $(0, \Delta s)$. Say the noise amplitude is $\Delta s/10$. Then the chaotic saddles with gap sizes in $(\Delta s/10, \Delta s)$ are immune to noise, yet their channel capacity is only slightly less than that of the original chaotic attractor. There are an infinite number of codes that can generate chaotic saddles with gap sizes in $(\Delta s/10, \Delta s)$. From the standpoint of channel capacity and noise resistance, these codes

are optimal. Similar results appear to hold for two-dimensional chaotic systems.

ACKNOWLEDGMENTS

We thank C. Grebogi and S. Hayes for discussions. E.B. was supported by the Army Research Labs and by the NSF under Grant No. DMS-9704639. Y.C.L. was supported by the NSF under Grant No. PHY-9722156, and by the University of Kansas.

-
- [1] S. Hayes, C. Grebogi, and E. Ott, Phys. Rev. Lett. **70**, 3031 (1993); E. Rosa, S. Hayes, and C. Grebogi, *ibid.* **78**, 1247 (1997); E. Bollt and M. Dolnik, Phys. Rev. E **55**, 6404 (1997).
- [2] S. Hayes, C. Grebogi, E. Ott, and A. Mark, Phys. Rev. Lett. **73**, 1781 (1994).
- [3] C. E. Shannon and W. Weaver, *The Mathematical Theory of Communication* (The University of Illinois Press, 1964).
- [4] R. E. Blahut, *Principles and Practice of Information Theory* (Addison-Wesley, New York, 1988).
- [5] R. C. Adler, A. C. Konheim, and M. H. McAndrew, Trans. Am. Math. Soc. **114**, 309 (1965).
- [6] It should be noted that $h_T = \ln 2$ is not a proof that a system is random since deterministic chaotic systems may also have a topological entropy of $\ln 2$. For instance, the topological entropy of the logistic map at $r=4$ is equal to $\ln 2$, but the logistic map is deterministic.
- [7] E. Bollt, Y.-C. Lai, and C. Grebogi, Phys. Rev. Lett. **79**, 3787 (1997).
- [8] E. N. Lorenz, J. Atmos. Terr. Phys. **20**, 130 (1963).
- [9] K. Cuomo and A. V. Oppenheim, Phys. Rev. Lett. **71**, 65 (1993).
- [10] This assumption is valid only when symbolic dynamics is investigated for fixed control parameter values. Nevertheless, when a bifurcation diagram is studied, there is a big difference between the logistic map and the Lorenz system. For instance, the logistic map generates a period-doubling cascade as a route to chaos, which is not observed on the Lorenz map.
- [11] The PIM triple method [H. E. Nusse and J. A. Yorke, Physica D **36**, 137 (1989)] is specially designed for computing a continuous trajectory on chaotic saddles existing in a given region for a diffeomorphism $\mathbf{F}: \mathbf{R}^2 \rightarrow \mathbf{R}^2$. A PIM (proper interior maximum) triple is three points (a, c, b) in a straight line segment L such that the interior point c (i.e., c is between a and b) has an escape time (time for leaving the region) that is larger than the escape times of both a and b . That is, (a, c, b) has a proper interior maximum. The idea is to find a sufficiently small triple and iterate the three points on the triple. The steps of the PIM triple procedure are as follows. (1) Specify a region of interest. If there is (are) attractor(s) coexisting in the region, isolate the attractor(s) with circles of appropriate radii. If a trajectory asymptotes to any attractor, this trajectory is considered to have escaped from the region. (2) Choose a line segment L_0 in the above region that straddles the stable manifold of the chaotic saddle. Distribute uniformly a number (say, 30) of points on the line segment and calculate the escape time for each point. Choose any PIM triple (a, c, b) from the 30 points. There are often many PIM triples that can be selected. One PIM triple can be chosen at random, or one can choose one systematically, choosing c to have the largest escape time. (3) Use the PIM triple as the new line segment and repeat step (2) until the length of the PIM triple so obtained is less than, say, 10^{-9} (denoted by I_0). Write $I_0 = R(L_0)$, that is, I_0 is our refined L_0 . (4) Iterate the end points of I_0 forward under the map. The two images are end points of a new segment denoted by L_1 . If the length of L_1 exceeds 10^{-9} , we apply step (2) until its length is less than 10^{-9} and we then replace L_1 by $R(L_1)$. (5) Repeat step (3) to find a sequence of PIM-triple intervals $[L_n]_{n \geq 0}$. (6) Write \mathbf{x}_n for the midpoint of L_n . It follows that $\mathbf{x}_{n+1} = \mathbf{F}(\mathbf{x}_n) + \varepsilon_n$, where ε_n is typically on the order of 10^{-9} .
- [12] For chaotic sets arising in two-dimensional invertible maps, every point on the set has a stable and an unstable direction. Distances along the stable (the unstable) direction shrink (expand) on the average exponentially in time. A chaotic set is hyperbolic if there is a stable and an unstable direction at each point of the set, and the angle between them is bounded away from zero. Otherwise the set is nonhyperbolic. In general, non-hyperbolicity is a complicating feature because it can cause fundamental difficulties in the study of the chaotic systems, a known one being the shadowability of numerical trajectories by true trajectories [see, for example, C. Grebogi, S. M. Hammel, and J. A. Yorke, J. Complexity **3**, 136 (1987); Bull. Am. Math. Soc. **19**, 465 (1988); C. Grebogi, S. M. Hammel, J. A. Yorke, and T. Sauer, Phys. Rev. Lett. **65**, 1527 (1990); T. Sauer and J. A. Yorke, Nonlinearity **4**, 961 (1991)].
- [13] P. Grassberger, H. Kantz, and U. Moenig, J. Phys. A **22**, 5217 (1989).
- [14] M. Hénon, Commun. Math. Phys. **50**, 69 (1976).
- [15] P. Cvitanovic, G. Gunaratne, and I. Procaccia, Phys. Rev. A **38**, 1503 (1988).
- [16] To our knowledge, at present numerical methods for finding continuous trajectories on chaotic saddles in maps of dimension three and higher remain uninvestigated.
- [17] C. Robinson, *Dynamical Systems: Stability, Symbol Dynamics, and Chaos* (CRC Press, Ann Arbor, 1995).
- [18] In general, there is at best a semiconjugacy of a symbol space onto an interval, since symbol spaces are totally disconnected, and intervals are connected. The relationship between the logistic map f_4 and its symbolic dynamics is only a semiconjugacy, but there is almost a full conjugacy. The problem occurs on only a countable set of points, the preimages of the symbol partition, $\cup_{i=0}^{\infty} f^{-i}(c)$. The logistic map is almost everywhere two-to-one, except at these points, and the full shift map is everywhere two-to-one. The ambiguity is between 0100... and

- 11 000 \cdots , for the “correct” symbol representation of the point $c = \frac{1}{2}$. However, there is a conjugacy between the logistic map f_4 , and the subshift Σ' consisting of the full shift Σ in which all symbol sequences of the form $\sigma_0\sigma_1\cdots\sigma_k01000\cdots$ (a preiterate of 01000 \cdots) are identified with $\sigma_0\sigma_1\cdots\sigma_k11000\cdots$ [see, for example, R. L. Devaney, *An Introduction to Chaotic Dynamical Systems*, 2nd ed. (Addison-Wesley, Redwood City, CA, 1989)]; i.e., we close the “gaps,” in the symbol representation.
- [19] G. Dahlquist and A. Björck, *Numerical Methods* (Prentice-Hall, Englewood Cliffs, NJ, 1974).
- [20] P. Collet and J.-P. Eckmann, *Iterated Maps on the Interval as Dynamical Systems*, Progress in Physics Vol. I (Birkhäuser, Boston, 1980).
- [21] B.-L. Hao, *Elementary Symbolic Dynamics and Chaos in Dissipative Systems* (World Scientific, Singapore, 1989).
- [22] See, for example, K. Aligood, T. Sauer, and J. A. Yorke, *Chaos, an Introduction to Dynamical Systems* (Springer, New York, 1997).
- [23] W. de Melo and S. van Strein, *One-Dimensional Dynamics* (Springer-Verlag, New York, 1992).
- [24] J. Milnor and W. Thurston, *On Iterated Maps of the Interval I and II* (Princeton University Press, Princeton, 1977). See also, J. Guckenheimer and P. Holmes, *Nonlinear Oscillations, Dynamical Systems, and Bifurcations of Vector Fields* (Springer-Verlag, New York, 1983).
- [25] A. N. Kolmogorov and S. V. Fomin, *Introductory Real Analysis* (Dover Publications, New York, 1970).